

# We are IntechOpen, the world's leading publisher of Open Access books Built by scientists, for scientists

**4,800**

Open access books available

**122,000**

International authors and editors

**135M**

Downloads

Our authors are among the

**154**

Countries delivered to

**TOP 1%**

most cited scientists

**12.2%**

Contributors from top 500 universities



**WEB OF SCIENCE™**

Selection of our books indexed in the Book Citation Index  
in Web of Science™ Core Collection (BKCI)

Interested in publishing with us?  
Contact [book.department@intechopen.com](mailto:book.department@intechopen.com)

Numbers displayed above are based on latest data collected.

For more information visit [www.intechopen.com](http://www.intechopen.com)



# Greenhouse Gases Reforming and Hydrogen Upgrading by Using Warm Plasma Technology

*Joel O. Pacheco-Sotelo, Ricardo Valdivia-Barrientos  
and Marquidia Pacheco-Pacheco*

## Abstract

Global warming is an alarming problem with adverse impact on climate change. Carbon dioxide (CO<sub>2</sub>) and methane (CH<sub>4</sub>) have been identified as the most significant greenhouse gases (GHG) normally arising from anthropogenic activities; therefore, promising treatment technologies are developing all over the world to resolve this problem. The warm plasma is an emergent process with low specific energy requirement capable to reach high temperature to produce excited species and support subsequent chemical reactions. Consequently, warm plasma reactors can be accomplished with simple structure reactors having high gas flow rates and treatment capacity. Plasma interaction with GHG leads into a molecular dissociation, mainly forming CO and H<sub>2</sub>, also known as syngas, which represents an alternative energy source with innovative applications in microturbines and fuel cells, among other emerging applications. The process here explained assures a significant reduction in CO<sub>2</sub> emission and H<sub>2</sub> yield upgrading. The reforming experimental results by using two warm plasma reactors are connected in series to improve the syngas yield. This alternative represents a great possibility for CO<sub>2</sub> conversion.

**Keywords:** warm plasma reforming, overall energy, H<sub>2</sub> upgrading

## 1. Introduction

Fossil fuels present a serious dilemma to humanity; around 86% of the world energy demand emanates from this source, having strong implications for global climate change. During the combustion of a ton of coal, more than 3.5 ton of CO<sub>2</sub> is released, which means an accumulation of 10<sup>12</sup> tons in the atmosphere [1]. An important parameter that determines the progress level of a country is the Human Development Index (HDI) [2], which considers the energy consumption expressed in kg oil equivalent per capita. This index is also used to establish the quality of life in a country, but this is paradoxical because to achieve a good standard of living, an immoderate consumption of energy is required; an inhabitant of the USA spends up to ten times more energy than another of Ethiopia; it means that this devastating energy consumption will revert in short term toward a poor quality of life.

The concentration of CO<sub>2</sub> has dramatically increased over the past 1000 years and can be explained by the industrialization and urbanization, as well as the indiscriminate use of fossil fuels and the consequent deterioration of natural

resources, representing a serious environmental, social, and economic problem [3, 4]. The average temperature on Earth's surface has also increased since the industrial revolution, notably in the last 50 years, and especially in recent decades, a significant increase in GHG concentration has been identified. Particularly in May 2013, the Mauna Loa Observatory (US NOAA) detected an alarming amount surpassing 400 ppm of CO<sub>2</sub>. This disquieting growth marked in just a few decades exceeds what has been accumulated in the atmosphere for over the last half million years, affecting the increasing average temperature of the planet [5]. Continuing in this way, the environmental consequences will have an irreparable cost and will probably reach a point where any living being will face serious problems.

GHG are the major cause of global warming; their average concentration is shown in **Table 1**. CO<sub>2</sub> has also has a long life in the atmosphere (between 5 and 200 years).

To find a new and better technology for CO<sub>2</sub> conversion, it is necessary to contemplate the energy cost and its impact on the environment. The reduced energy content in CO<sub>2</sub> represents the main limitation for a posterior reuse, demanding additional energy, which eventually impacts on new CO<sub>2</sub> emissions. Consequently, the energetic cost involved in its reuse must consume less energy than that obtained at the termination of the process. The most effective and cost-free way to collect and transform CO<sub>2</sub> is provided by nature itself through the well-known process of photosynthesis [7]; however, human being has not been capable to adapt this process to a feasible technology, except by providing extra energy of the order of 191 MJ/kg to obtain H<sub>2</sub> having an energy value of 120 MJ/kg; to be specific, a deficiency still remains in the energy cost.

Concerning wind energy, it is characterized by the complete absence of GHG emissions being one of its main advantages; nevertheless, it is a variable energy source with a stochastic pattern that is difficult to predict, which implies adding storage services and requiring installed in spaces close to the coast or on maritime platforms. The requirement of storage units leads to a temporary inertia in the loading and unloading, so it may not always be available for transitory energy demands.

Regarding the energy derived from biomass (referred as bioenergy), it still has numerous challenges: natural vegetation has to be sacrificed with a massive deforestation to produce crop-based biofuels to make available their growing demand [8].

Nuclear energy is also another primary source of energy that can be considered clean in terms of CO<sub>2</sub> emissions, which currently produces 17% of world consumption (2700 TWh). A global plan in the medium or long term consists in the

Constituent	Concentration
CH <sub>4</sub>	55–70% vol
CO <sub>2</sub>	30–45% vol
N <sub>2</sub>	0–2% vol
COV	0% vol
H <sub>2</sub> S	>500 ppm
NH <sub>3</sub>	~100 ppm
CO	~100 ppm
Siloxanes	~100 ppm
Lower heating value (LHV)	~22.5 MJ/m <sup>3</sup>

**Table 1.**  
GHG average concentration [6].

transition from thermal power plants to nuclear power plants, since a significant reduction in GHG emissions, notably CO<sub>2</sub>, is ensured. In Europe, the total electricity produced by the nuclear route reaches 80% in France, 60% in Belgium, and 43% in Sweden. Therefore the transition to this alternative could occur in short term taking advantage of the GHG energy capacity.

An additional energy source is hydrogen. Hydrogen is considered as the fuel of the stars, because in our Sun, every second 600 million tons of hydrogen are converted into helium only by nuclear fusion, releasing enormous amounts of energy, providing also the light and heat which makes life on Earth possible.

It is imperative to ask if it is reasonable to use fossil fuels to generate electricity and then use the electricity to generate hydrogen. Each transformation involves energy losses, thus the overall efficiency becomes lower and, furthermore, CO<sub>2</sub> would be emitted to the atmosphere. In order to be sustainable and environmentally friendly in the long term, electricity for water electrolysis must be derived from renewable or nuclear energy sources which do not emit CO<sub>2</sub> and air pollutants, such as SO<sub>2</sub> and NO<sub>x</sub>. Hydrogen is also very attractive as a fuel or additive for internal combustion engines, because it can considerably reduce air pollution; however, using H<sub>2</sub> as a fuel for vehicles requires large high-pressure containers or cryogenic vessels if it is compressed as liquid. This problem can be eliminated by installing on board a plasma reactor to produce hydrogen-rich gas. Gaseous or liquid hydrocarbon fuels are converted by plasma reactor producing hydrogen-rich gas. The efficiency of the overall system is attained by an energy balance when a mixture of hydrocarbon fuel combined with hydrogen-rich gas is injected into the engine.

The energy emitted by the Sun is the most abundant primary source, providing 10,000 times more energy than the total consumption in the world, the terrestrial atmosphere receives a power density of 1370 W m<sup>-2</sup>, the direct transformation to electrical energy is achieved through solar cells, which are noiseless, do not generate emissions, do not consume fuel, have simple installation, do not have moving parts, and are easy to maintain. However, the main challenge is its temporary storage dependence of energy to supply the variations (or absence) of solar radiation, which increases its operating cost at an order of magnitude higher than generation by natural gas.

In recent years the carbon capture and conversion (3C) technology has been emerging with a greater scope, which, unlike the carbon capture and storage (CCS), does not treat CO<sub>2</sub> as a waste, but on the contrary, promotes its conversion to industrial uses.

Natural gas or biogas reforming are considered cleaner than coal gasification in most countries but is facing technological challenges because the catalysts are inclined to deactivation by soot deposition and sulfur poisoning. In mitigation of these issues, plasma-based CO<sub>2</sub> dissociation technologies could probably offer a new alternative for syngas production.

In recent times many topics are conveniently changing from “control” to “utilization”—using CO<sub>2</sub> and other greenhouse gas for new applications; for existent conditions it is difficult to control or prevent new CO<sub>2</sub> emissions, searching its utilization as raw gas in obtaining further substances is much easier under special conditions. Then, CO<sub>2</sub> becomes a useful gas rather than only a GHG.

Actually, the syngas reforming into methanol or other liquid fuels use the well-known Fischer-Tropsch (FT) processes normally assisted by catalysts; however, this leads to the following disadvantages:

- a. Several compressors are required to achieve a pressure of 20–80 bar is required to realize diffusion through the membranes or to attain the operating ranges in the FT process.

- b. Temperatures between 200°C and 500°C are needed in syngas reforming. At these temperatures large amounts of steam are generated, which subsequently limit the catalyst activity and deposit carbon layers on its surface reducing its lifetime and dipping its conversion capacity.
- c. Catalysts are vulnerable to sulfur compounds and therefore require regeneration or replacement cycles. The catalyst depends on the specific surface area, being the most commercial and accessible catalysts of those made of CuO and Al<sub>2</sub>O<sub>3</sub>. The Pd catalysts present better performance but have higher economic cost.
- d. Contact time between catalysts is crucial to obtain liquid fuels; consequently it is necessary to limit the gas flow at reduced ranges, which leads to high residence times.
- e. H<sub>2</sub>/CO<sub>2</sub> and CO/CO<sub>2</sub> ratios are optimum when they approach to 2; steam is generated at higher ratios. By exceeding these optimal relations, steam is generated, and excessive water could deactivate the catalyst action, and a reverse reaction also occurs (WSR).

In the case of conventional steam reforming of CH<sub>4</sub> or natural gas, it requires 4.5 kg of H<sub>2</sub>O for each kg of H<sub>2</sub> produced, but 5.5 kg of CO<sub>2</sub> is released. When using the reformed coal, 3 kg are required for every 9 kg of water and 11 kg of CO<sub>2</sub> are released, so the latter is considered the most polluting of the processes.

Once H<sub>2</sub> is generated by different processes, it is important to consider its compression, liquefaction, transport, and storage, taking into account its physical properties ( $\rho_{\text{gas}} = 0.088 \text{ kg/m}^3$ ,  $\rho_{\text{liquid}} = 70 \text{ kg/m}^3$ ), and boiling point of 20.3 K. So the energy needed to produce, compress, liquefy, transport, transfer, and store H<sub>2</sub> plus the losses in each conversion added to the process of reversion to electrical energy (through a fuel cell with 50% conversion) in each of the stages can reach to consume more energy than that it will provide or recover from H<sub>2</sub>. In addition to the energy cost, another factor to consider is the economic factor: each GJ of H<sub>2</sub> costs \$5.6 when it is obtained from natural gas, goes up to \$10.30 when using coal, and costs \$20.10 with water electrolysis; in this last the consumption of electricity represents 79% of the deliverable energy cost of H<sub>2</sub> (140 MJ/kg) [9].

A short-term alternative is to use a primary source of energy, in this case GHGs or biogas resulting from biodigester and its treatment with plasma to obtain syngas. The provisional storage of this chemical energy contained in the syngas represents a viable alternative either for its “a posteriori” reversion or for its direct reversion “in situ” to electrical energy using fuel cells.

## 2. General plasma characteristics

A fundamental principle differentiating the plasma's behavior from other fluids is that each charged particle simultaneously reacts with a considerable number of charged particles, thus producing an important collective effect. The range of temperatures comprised by laboratory plasmas ranges from room temperature to temperatures comparable to those found inside stars, while density range expands from 10<sup>12</sup> to 10<sup>25</sup> m<sup>-3</sup>; it should be noted that plasmas of industrial interest have kinetic temperature range comprised from 1 up to 20 eV.

Plasma gas discharges are characterized by its chemical activity convenient to induce chemical reaction even without catalyst requirement, that is, plasma

discharges act as a thermochemical reactor overcoming many particular problems in catalytic reformers such as short lifetime, expansive costs, and slow-moving time response. Plasma gas discharges are divided into two types according to its temperature and electron density: nonlocal thermodynamic equilibrium and local thermodynamic equilibrium. In the first case, the degree of particle ionization is very weak, and the temperature of electrons is much higher than heavy particles, so the ion temperature is low and is recognized as cold plasma. Crown plasma dielectric barrier discharges are examples of this category of plasmas where reactions with radicals are common. In the second case, a higher degree of particle ionization, higher electron density, and comparable temperatures in heavy particles and electrons are characterized. This kind of plasma is produced by transferred electric arcs, plasma torches, and high-intensity radio frequency discharges.

A third category or a category having conventional thermal plasma and non-equilibrium plasma conditions is the warm plasma. The warm plasma is a transitional discharge able to work under moderate power density at enough high gas temperature to produce molecule dissociation and excited species, supporting the subsequent chemical reactions. Such plasma discharges have significant advantages: The reactor has simple assembly and do not require extra cooling systems, since they work with reduced electric currents and high voltages; consequently the electrode erosion is notably diminished. Warm plasmas are also characterized by high chemical selectivity and have found applications in fuel conversion to syngas production, hydrogen sulfide dissociation, and CO<sub>2</sub> dissociation. Gliding arc plasma discharge or jet atmospheric pressure plasmas are examples of warm plasma discharges.

Therefore, the use of warm plasma is considered more appropriate to treat GHG because the syngas gas formed by H<sub>2</sub> and CO molecules still exists in temperature range 900 up to 3500 K, just for our application interest (see **Figure 1**). The cold plasma having a lower range of temperatures also reaches the dissociation of GHG but does not subsist stable when relatively high GHG flows rates are treated.

The ionization process in warm plasma discharges are induced by a strong electric field, producing relatively high-energy particles, leading in selective chemical transitions in a very effective manner, and subsequently, the energy necessary to support the electric discharge is reduced, since the electrical conductivity  $\sigma(T)$  has a stepwise behavior and the internal wall temperature of the reactor is kept high reducing the radiation losses.

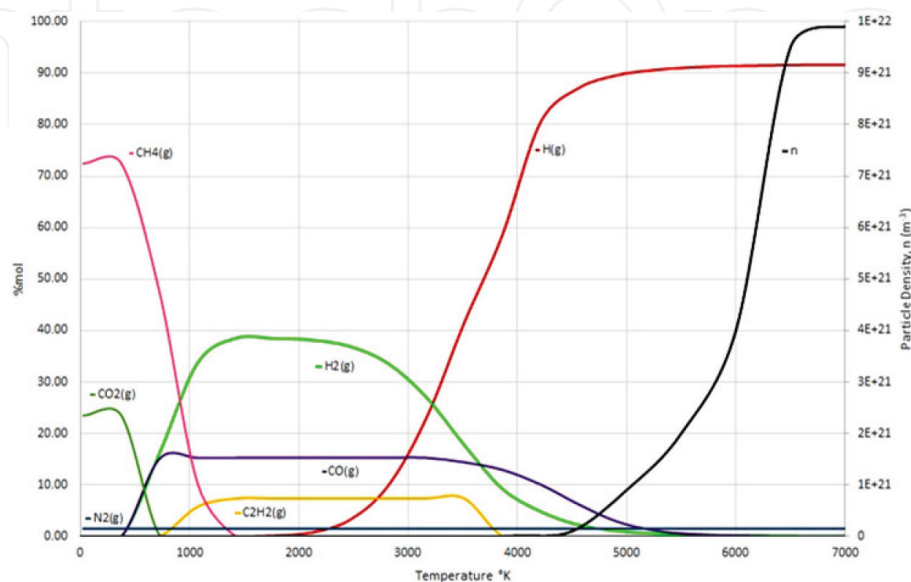


**Figure 1.**  
GHG concentration variation in function of temperature.

Because of its high power density, this plasma reactors can be designed for small- and large-scale applications, these types of reactors can also work in portable or onboard processes [10]. In summary, the use of warm plasma is more adequate for our purposes.

The HSC software [11] combines chemical and thermodynamic features enabling calculations in standard computer to visualize conversion and yielding data in function of temperature or other input variables. So the prediction of important results and confirmation of experimental ones can be attained. With regards to biogas concentrations shown in **Table 1**, the HSC was used to simulate and find the evolution of the participating species (reactants and by-products) that are carried out in a temperature range of 300–7000 K. **Figure 3** shows a maximum H<sub>2</sub> yield in the temperature range 1200–2600 K. Another diatomic species is C<sub>2</sub>H<sub>2</sub> whose concentration begins to increase at 1000 K, remains at a constant maximum value up to 3000 K, and then decays and dissociates to monatomic species. Other species not marked in **Figure 3** are the radicals N<sup>+</sup>, OH, C<sup>+</sup>, as well as the concentration of electrons, which begin to increase considerably from 4000 K. Enough information on this monoatomic or radical species can be found in Ref. [12]. Regarding the electron density n<sub>e</sub>, it has a significant increase beyond 5000 K, consequently corresponding to thermal plasmas discharges.

Additionally, warm plasma discharges are characterized by a good energy efficiency transfer principally because an efficient vibrational excitation of the molecules can be reached, and this leads in a better molecule splitting with less energy insertion. The selective excitation of vibrational modes enhances the chemical selectivity, because it requires a low amount of electron energy to increase the lowest vibrational level, and by interchanging this energy with other vibration levels (VL) this leads in a concentration increase of the higher levels to finally get the vibrational-vibration relaxation (V-V) up to reach a dissociation level, allowing as a result, reduced energies, diminishing from 10 to only 5.5 eV. The selective mechanism consists in sending electrical impulses into the plasma discharge, and once the dissociation has been achieved, the reactions can be sustained by applying a lower energy of around 1 eV/mol [13, 14]. As a consequence the chemical reaction is carried out in a shorter time and with reduced energy cost, specifically if a vibrational excitation is promoted.

The most important characteristic of CO<sub>2</sub> is its high specific heat at lower temperatures that significantly increases the enthalpy; therefore, a more constricted arc is produced, and as a consequence a higher current density is produced, hence a higher magnetic pinch pressure and a higher plasma flow velocity are manifested.

Compared to traditional catalytic reforming processes with high capital costs, high temperature requirements, large equipment size, and rapid loss of catalyst activity [15, 16], warm plasma reforming (WPR) would provide an attractive route for methanol reforming, because the gas temperature can be low, while the electrons are highly energetic to sustain the chemical reactions.

## 2.1 High-frequency operation effect

The importance of high-frequency (HF) plasma discharge and its effect in V-I relationship behavior is presented in this section, indicating a more stable discharge once higher frequency is applied into discharges.

Since the warm plasma discharge is a complex physical concept, the mathematical equations describing an exact physical behavior would be very difficult to obtain and even more difficult to solve; so an approximate and manageable model of the plasma discharge derived from the well-known Elenbaas-Heller equation, considering constant pressure and others simplifications as was explained elsewhere

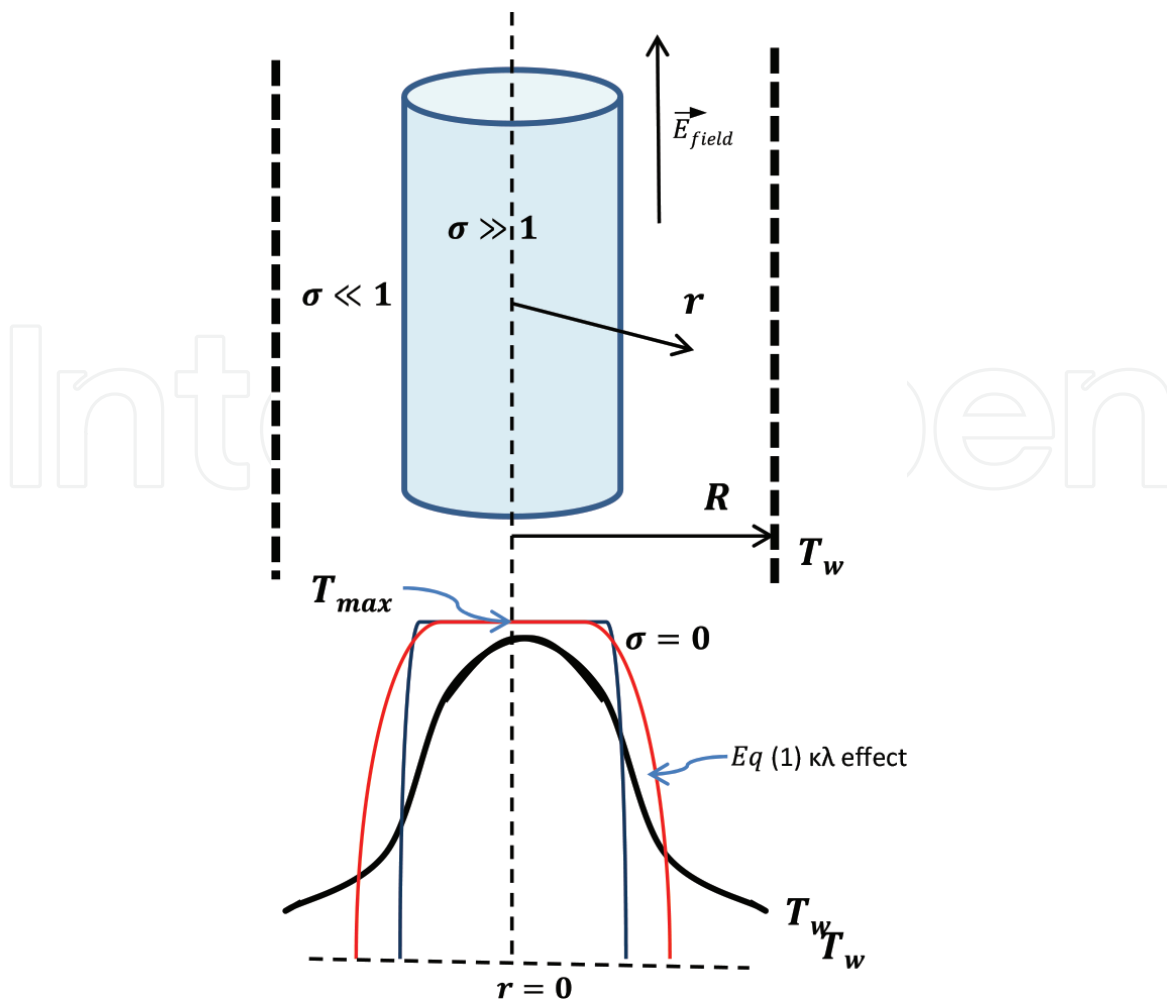


**Figure 2.**  
 Temperature profile according electrical conductivity.

[17, 18], is expressed in Eq. (1); this model is taken up again to demonstrate the effects of the frequency on the discharge stability.

The electric field applied ( $E_{field}$ ) in the discharge column (see **Figure 2**) gives the power transmitted to the electrons and then transferred to the gas atoms via elastic and inelastic collisions among electrons, atoms, and other species participating in the discharge. Consequently, the gas is heated up, and the thermal energy is removed by thermal conduction, radiation, convection, and diffusion.

In warm plasma, the radiation and convection losses are neglected because no intense current participates in discharge, so Eq. (2) is obtained:

$$\rho C_p \frac{dT}{dt} = \sigma E^2 + \frac{1}{r} \frac{d}{dr} \left( \frac{\kappa dT}{dr} \right) \quad (1)$$

$$\frac{dT}{dt} = \frac{\frac{I_{disch}^2}{S \sigma(T)} - [P_{loss}]}{S \rho(T) C_p(T)} \quad (2)$$

This algorithm uses an initial temperature value to calculate the Joule power loss  $P_{loss}$ , and the specific heat  $C_p(T)$ , the density  $\rho(T)$ , and the discharge electrical conductivity  $\sigma(T)$  are obtained from a database for a given constant pressure [19].  $S$  represents the transversal section of the column discharge. Once these coefficients have been determined, it is possible to solve this equation by using a SIMULINK tool and presenting the discharge as a two-terminal electrical device. This model accomplishes a good agreement between analytical and experimental values at low



and high frequencies, moreover it allows us to find the characteristic discharge time and temperatures of plasma (see Section 2.2).

The manner in which the discharge impedance responds as a component of the circuit is a key element that describes the discharge behavior, and its interaction with the power supply, subsequently, is a very useful tool to design an efficient converter-discharge system. The model also shows that the temperature modulation in the discharge decreases considerably according to the relaxation time and predicts the discharge electrical behavior, considering different power requirements at high and low frequencies.

## 2.2 Relaxation time and frequency effect

When the source of energy in (1) is extinguished, the right first term equals zero ( $E = 0$ ); in consequence the temperature begins to decay, resulting in a simple Eq. (3), leading an expression for the relaxation time  $\tau_{rel}$  (4):

$$\rho C_p \frac{dT_0}{dt} + 4 \left( \frac{\kappa T_0}{r^2} \right) = 0 \Rightarrow \frac{dT_0}{dt} + \frac{4\kappa T_0}{\rho C_p r^2} = 0 \quad (3)$$

$$\Rightarrow T_0(t) = T_i e^{-t/\tau_{rel}} \left\{ \begin{array}{l} T_i = \frac{EI}{4\pi\kappa} \\ \tau_{rel} = \frac{\rho C_p \pi r^2}{\kappa 4\pi} \end{array} \right. \quad (4)$$

Thus, the dynamic behavior is similar to a first-order circuit. The relaxation time depends inversely on the thermal conductivity  $\kappa$  and directly on the density  $\rho$  and specific heat  $C_p$ , as well as on the radius of the discharge, which for practical purposes has been considered to be 0.4 mm. In this manner, the family of curves expressed in **Figure 3** can be obtained.

It is obvious that  $\text{CO}_2$  has the highest relaxation times ( $\sim 200$  ms) and  $\text{H}_2$  presents the lowest conductivity times ( $\sim 200$   $\mu\text{s}$ ) as a consequence of its remarkable

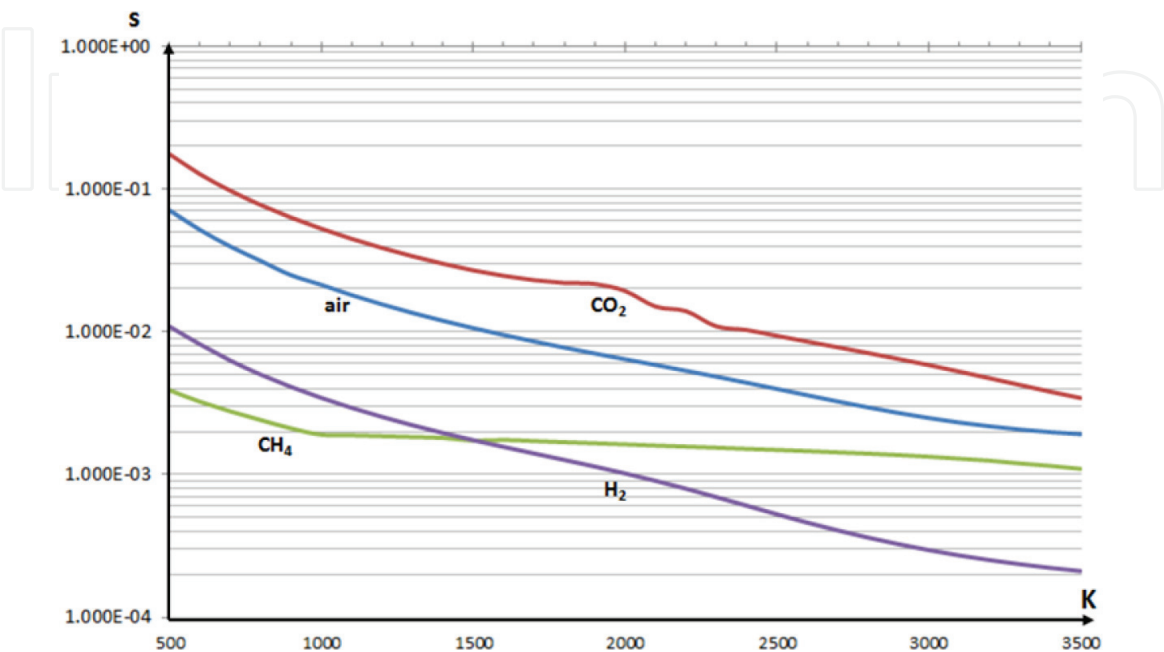


**Figure 3.**  
Discharge plasma relaxation time.

thermal conductivity. Above 1500 K, H<sub>2</sub> has a shorter relaxation time, which means that heating and cooling time is less than the rest of the gases in the plasma discharge, so it is convenient to apply a discharge frequency greater than 10 kHz, as a consequence the temperature variations will be reduced, as shown in thermal stress simulation at different frequency operations in **Figure 4**.

Another useful parameter is the temperature modulation of the plasma which relates the temperature variations of a discharge respect its average temperature as a function of the frequency of operation  $[(\Delta T/T_{av})_f]$ ; [20] defines temperature variations and average temperature as

$$\Delta T = \frac{T_{max} - T_{min}}{2} \quad (5)$$

and

$$T_{av} = \frac{T_{max} + T_{min}}{2} \quad (6)$$

The temperature variations and average temperature in function of frequency were determined from Eqs. (5) and (6), and its results are depicted in **Figure 4**. At frequencies beyond 5 kHz, the temperature variation is approximately 1% around a temperature value of 3900 K, while for a low frequency such as 50 Hz, the temperature variation corresponds to almost 1500 K. Therefore the influence of the frequency respect to the supply current in plasma discharge is closely connected with the relaxation time  $\tau_{rel}$  during plasma freshening [21, 22]. In conclusion, if the waveform signal period exceeds this relaxation time, the plasma temperature will be modulated (50 Hz case in **Figure 4**). In the opposite case, when the period is much lower than  $\tau_{rel}$  as in the case of HF (>5 kHz), the plasma temperature will be nearly constant. A free decay temperature arises when the plasma discharge is turned off, indicative of the thermal discharge response to changes in waveform signal source.

By using the same model, the V-I relationship of an electrical discharge can be obtained and represented as a Lissajous curve presented in **Figure 5**. Simulations were performed at different frequency values, starting at 50 Hz up to 5 kHz. When

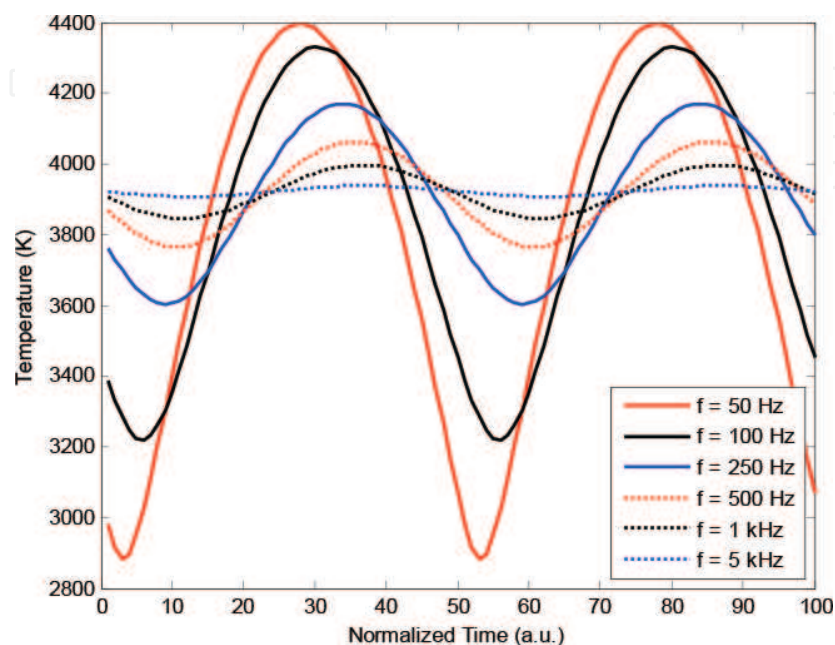


**Figure 4.**  
 Thermal stress at different frequency operation.

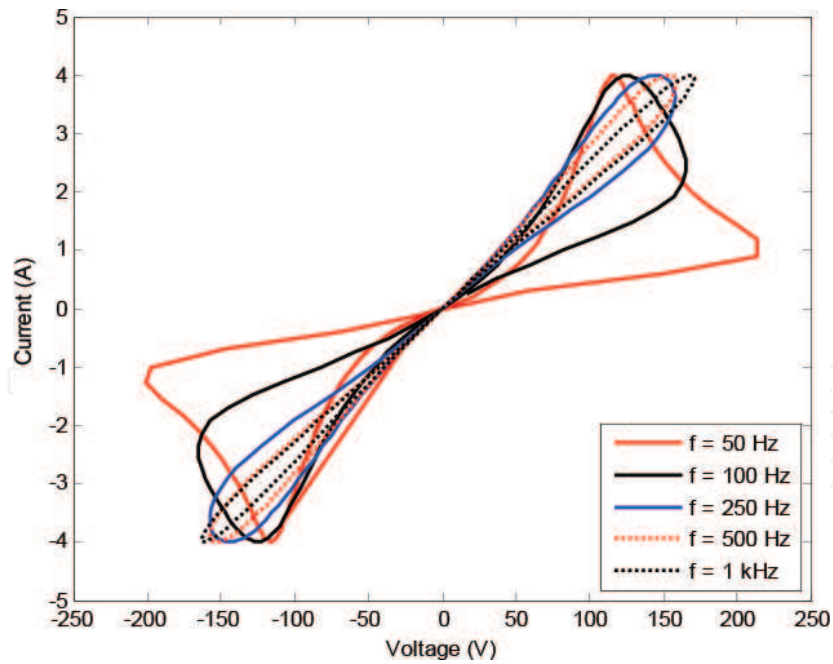


**Figure 5.**  
*V-I relationship and its frequency effect.*

the excitation frequency becomes relatively high ( $>5$  kHz), the discharge characteristic V-I behavior inclines to be completely linear, comparable to a purely resistance charge; otherwise, if the frequency is reduced ( $<100$  Hz), the discharge is nonlinear; for some points where the voltage is not large enough, at that time the discharge current will be extinguished and must wait for the next period to reach a voltage level high enough to ionize and restart the discharge, thus succeeding with high current impulsions, producing a noisy spectrum. In the case of direct current operation, the V-I operating area shows a static path having a slope  $\Delta V/\Delta I < 0$  so the behavior is very unstable, and to overcome this problem, a high series resistance must be included in the trajectory discharge, increasing the power loss and diminishing the efficiency.

### 2.3 Important parameters in reforming processes

There are numerous methods to generate syngas ( $H_2 + CO$ ) [23, 24]. These methods include steam reforming (SR), partial oxidation (POX), and dry reforming (DR), as shown in Eqs. (7)–(9):



The advantages of dry reforming (9), compared with the other procedures, include the use of  $\text{CO}_2$  and  $\text{CH}_4$  as reactants mixture; as is well known, this mixture represents 94% of the GHGs. The focus of this work includes the research of the warm plasma discharge, applied for GHG reforming; in addition the electrical energy cost is optimized to produce higher GHG conversion and to obtain a high yield and selectivity rates of  $\text{H}_2$ . However,  $\text{H}_2$  as a fuel has significant drawbacks, especially those related with its storage. Even though hydrogen has a high mass heating value ( $120 \text{ MJ kg}^{-1}$ ), it has a very low volumetric heating value ( $11 \text{ kJ l}^{-1}$ ),

compared for instance to  $16,000 \text{ kJ l}^{-1}$  for methanol. The ideal scenarios where DR might be considered are anywhere the supply of  $\text{CH}_4$  is linked with  $\text{CO}_2$ .

The general idea about DR technique consists in using the GHG into plasma discharge to produce higher energetic synthetic by-products ( $\text{H}_2 + \text{CO}$ ).

Usually in literature, two important parameters are utilized as good indicators for describing plasma dry reforming process efficiency. These parameters are specific energy (SE) and energy efficiency conversion (ECE).

SE represents the energy needed to produce a mole of syngas, according to Eq. (10):

$$\text{SE} = \frac{P_{el} t_{exp}}{\text{mol}(\text{H}_2 + \text{CO})_{\text{produced}}} \quad (10)$$

where  $P_{el}$  represents the discharge power applied for a time  $t_{exp}$ ; consequently it represents the energy applied and expressed in (kJ), and the denominator  $\text{mol}(\text{H}_2 + \text{CO})_{\text{produced}}$  denotes the syngas produced. The reformation process will have a better performance, whereas this rapport inclines to slight values of SE.

ECE signifies the proportion of energy contained in syngas obtained in relation to the input energy, which is the sum of the energy applied in the plasma ( $P_{el} t_{exp}$ ) and the energy during the  $\text{CH}_4$  conversion. ECE is defined by Eq. (11).

The most desirable ECE value must be close to 100%:

$$\text{ECE} = \frac{[(\text{mol H}_2 \text{ produced})(LHV_{\text{H}_2}) + (\text{mol CO}_{\text{produced}})(LHV_{\text{CO}})]}{P_{el} t_{exp} + [(\text{mol CH}_4 \text{ converted})(LHV_{\text{CH}_4})]} \times 100 \quad (11)$$

In order to calculate the ECE the LHV utilized are reported in **Table 2**.

Once the reaction takes place, in addition to SE and ECE, it is of great interest to know the reactants conversion, which is attained by using Eqs. (12) and (13), indicating the amount of  $\text{CH}_4$  and  $\text{CO}_2$  that are converted during the reaction:

$$\text{CH}_4 \text{ conversion}(\%) = \frac{\text{molCH}_4 \text{ converted}}{\text{molCH}_4 \text{ feed}} \times 100 \quad (12)$$

$$\text{CO}_2 \text{ conversion}(\%) = \frac{\text{molCO}_2 \text{ converted}}{\text{molCO}_2 \text{ feed}} \times 100 \quad (13)$$

The principal reaction by-products are  $\text{H}_2$  and  $\text{CO}$ ; the conventional manner to evaluate them is by using Eqs. (14) and (15). The  $\text{H}_2$  yield is defined as the ratio of  $\text{H}_2$  produced during the reaction in relation to the input  $\text{CH}_4$  multiplied by two, because each mole of  $\text{CH}_4$  produces 2 moles of  $\text{H}_2$ . Whereas  $\text{CO}$  yield is defined as the ratio of  $\text{CO}$  produced during the reforming in relation to the input of  $\text{CH}_4$  plus  $\text{CO}_2$ :

$$\text{H}_2 \text{ yield}(\%) = \frac{\text{mol H}_2 \text{ produced}}{2 \times \text{mol CH}_4 \text{ feed}} \times 100 \quad (14)$$

Molecule	LHV ( $\text{kJ mol}^{-1}$ ) @ 298.16 K
$\text{H}_2$	242.056
$\text{CO}$	283.179
$\text{CH}_4$	802.933
$\text{C}_2\text{H}_2$	376.5

**Table 2.**  
 LHV for different gases [25, 26].

$$\text{CO yield (\%)} = \frac{\text{mol CO}_{\text{produced}}}{\text{mol CH}_4_{\text{feed}} + \text{mol CO}_2_{\text{feed}}} \times 100 \quad (15)$$

Similarly, according to Ref. [25] the acetylene produced is given by

$$\text{C}_2\text{H}_2 \text{ yield (\%)} = \frac{2 \times \text{mol C}_2\text{H}_2_{\text{produced}}}{\text{mol CH}_4_{\text{feed}}} \times 100 \quad (16)$$

In the same way, the selectivity of these three products are defined by Eqs. (17)–(19):

$$\text{H}_2 \text{ selectivity (\%)} = \frac{\text{mol H}_2_{\text{produced}}}{2 \times \text{mol CH}_4_{\text{converted}}} \times 100 \quad (17)$$

$$\text{CO selectivity (\%)} = \frac{\text{mol CO}_{\text{produced}}}{\text{mol CH}_4_{\text{converted}} + \text{mol CO}_2_{\text{converted}}} \times 100 \quad (18)$$

$$\text{C}_2\text{H}_2 \text{ yield (\%)} = \frac{2 \times \text{mol C}_2\text{H}_2_{\text{produced}}}{\text{mol CH}_4_{\text{converted}}} \times 100 \quad (19)$$

Finally, the syngas relationship  $\text{H}_2/\text{CO}$  is determined by (20), this important parameter indicates the content of  $\text{H}_2$  in the syngas, and it could define the conversion processes in which it can be used to obtain successive by-products:

$$\text{H}_2/\text{CO (u.a.)} = \frac{\text{mol H}_2_{\text{produced}}}{\text{mol CO}_{\text{produced}}} \quad (20)$$

In the dry reforming technique, an ideal  $\text{H}_2/\text{CO}$  ratio close to 1 must be obtained, and this ratio can be easily modified by controlling the concentration of reactants at the inlet supply. Therefore, the syngas obtained from the dry reforming can be used in the synthesis of a variety of chemicals in much more extensive manners than in the other reforming processes. Another advantage of dry reforming is that  $\text{CO}_2$  content can be exploited in natural gas sources, biogases, coal-methane, and organic waste.

An alternative way to promote  $\text{CO}_2$  conversion is to mix this molecule with another substance, which usually has a higher Gibbs energy, such as  $\text{H}_2$  or  $\text{CH}_4$ , because it provides energy-carrying radicals that come from  $\text{H}_2$ . For instance, the reaction  $\text{CO}_2 + \text{H}_2 \rightarrow \text{CO} + \text{H}_2\text{O}$  ( $\Delta H_0 = +51 \text{ kJ mol}^{-1}$ ) requires almost six times less energy to promote the conversion of  $\text{CO}_2$  than that obtained when it is unmixed  $\text{CO}_2 \rightarrow \text{CO} + (0.5)\text{O}_2$  ( $\Delta H_0 = +293 \text{ kJ mol}^{-1}$ ). The vibrational energy is lower than that of electronic excitation, for example, for the  $\text{H}_2$ , 4.4 eV is required and for its electronic excitation the double of energy (8.8 eV).

Since biogas also contains unfavorable impurities ( $\text{H}_2\text{S}$ ,  $\text{NH}_3$ , chlorine, and siloxane compounds), a cleaning process is generally required for previous transportation or conversion. Commonly zeolite and carbon nanomaterial are used as adsorbents due to their excellent thermal stability, low cost, large specific area, and pore volume [27]. Noble metals working at high pressures like Pt, Pd, and Ru are also used, particularly because they are less sensitive to carbon deposition, but they are rather expensive in industrial high flow rate applications.

### 3. Experimental setup and warm plasma reactor features

The warm plasma reactor is constructed in a copper segmented configuration; the mixture gas enters tangentially into the reactor, as is depicted in **Figure 6**

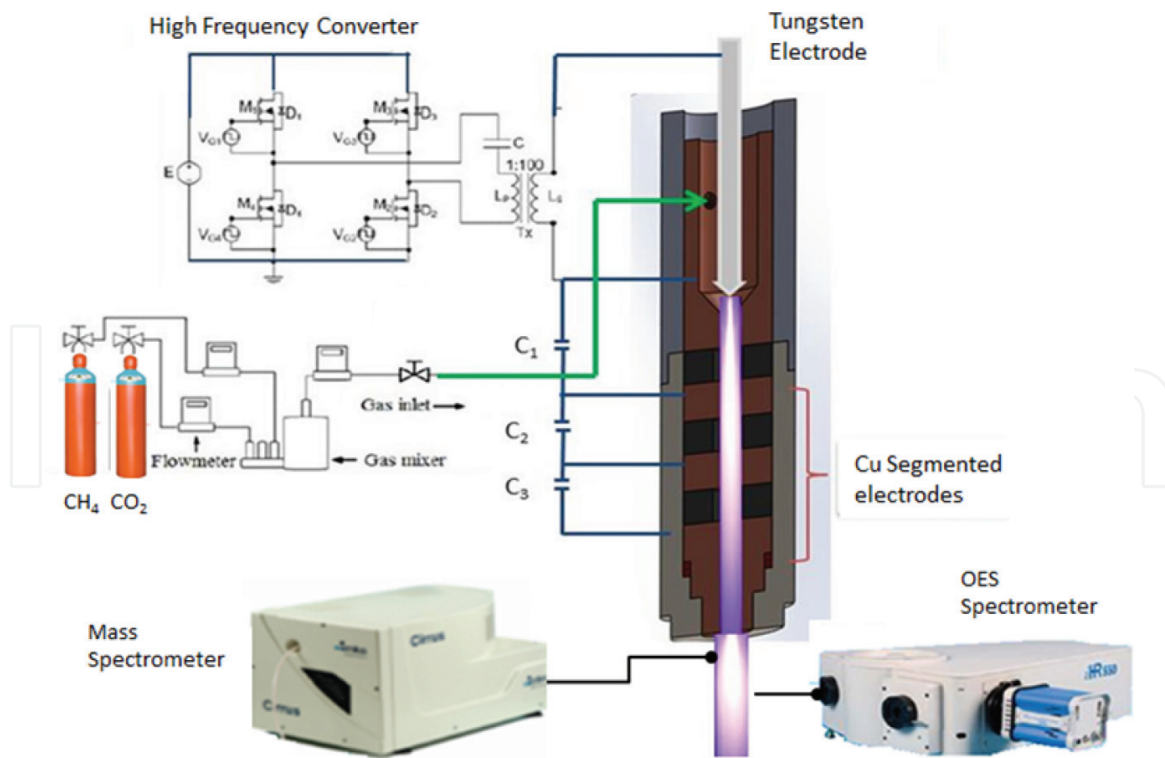


**Figure 6.**  
*Segmented plasma torch for GHG reforming.*

looking to preserve a stable temperature along the jet length and at the same time to preheat the GHG before entering to plasma discharge and thereby achieving a faster ionization. The plasma discharge is generated between an external electrode and a central tungsten electrode. Due to the different physical properties between central electrode (tungsten) and external electrode (copper), the role of cathode and anode is periodically alternating; as a result the current passes twice zero during a period of the supply voltage.

The flux moving through the segmented electrodes elongates the plasma jet with a large volume. The arc discharge continues the spiral motion descending along the chamber reactor increasing the column length, and also a swirl effect is formed enhancing the reaction time in the central part of the discharge. The whole plasma is confined to a post-chamber 1 cm in diameter and 12 cm in length. The voltage needed to initiate the discharge ranges from 8 up to 10 kV; once the plasma is started, the voltage automatically drops to a lower level (around  $2kV_{pp}$ ). The arc column length is a function of power applied to the discharge, reactor geometry, and nature of the gas to be treated.

Optimal experimental conditions were found to be 8–14 LPM, the power input for a stable discharge is in the 300–700 W depending on the gas to be treated. By adding nitrogen gas and increasing the power up to 500 W, the gas ionization through the entire length of the reactor is assured. N<sub>2</sub> addition in GHG's treatment leads to a better dissociation creating active species being dispersed homogeneously in the plasma reactor by causing the dissociation of the initial molecules by third body impact. Besides a third participant gas, N<sub>2</sub> promotes the dissociation of CH<sub>4</sub> by creating the radicals CN, C<sub>2</sub>, and CH, very useful for the route toward methanol synthesis [28].

The power source consists of a high-frequency full bridge converter constituted by one ferrite core setup transformer to provide up to 10 kV at high frequencies. The power supply handles a wide-frequency range operation (5–200 kHz). The duty cycle in each phase is adjusted to 50% providing a soft start in the MOS

avoiding redundant power consumption in the plasma discharge as it was explained in detail elsewhere [29]. The HF transformer transfers the maximum energy toward the plasma discharge; in addition, it also functions as a stabilizer, because a natural negative feedback controls the impedance plasma discharge; when the impedance charge goes down, the voltage is automatically adjusted to sustain a stable plasma discharge; and consequently a lower electrical field of about 3 kV/mm is applied between electrodes; as a result, a low-current discharge streaks between the electrodes' closest points and pre-ionizes the gas gap, causing the formation of a stronger current to sustain the warm plasma discharge in the GHG.

By working at HF, the fitting transformer size and weight are reduced as well for the other passive components becoming competitive in energetic and price terms. The transformer contains a ferrite core EI-shaped type, naturally protected against short circuit on the secondary coil because of the important leakage magnetic flux which allows obtaining an automatic impedance control. The simplified block diagram of the proposed converter (HF converter) is shown in **Figure 6**, which is a symbolic illustration of the internal modules and its connection with the plasma reactor.

#### 4. Experimental results

Some samples were taken directly from a biodigester. To achieve this sampling, a special compressor was used, to store the gas in a container through a pressure up to 300 kg cm<sup>-2</sup> (see **Figure 7**). The diagnosis reveals that some impurities such as H<sub>2</sub>O, H<sub>2</sub>S, H<sub>2</sub>O, air, etc. were counted in in the biogas, being the principal components CH<sub>4</sub> as is exposed in **Table 3**.

Preserving the concentrations obtained in the biogas characterization, the mixture of these gases was injected in the experimental arrangement shown in **Figure 6**, with an applied power of 461 W throughout 143 s of experiment duration,



**Figure 7.**  
*Biogas sampling.*

Specie	Concentration (% vol)
CH <sub>4</sub>	55.7200
CO <sub>2</sub>	13.4900
Air	28.2200
H <sub>2</sub> S* 236 ppm	* 0.0236
H <sub>2</sub> O	1.3480
Other species	1.1984

**Table 3.**  
*Biogas mixture concentration.*

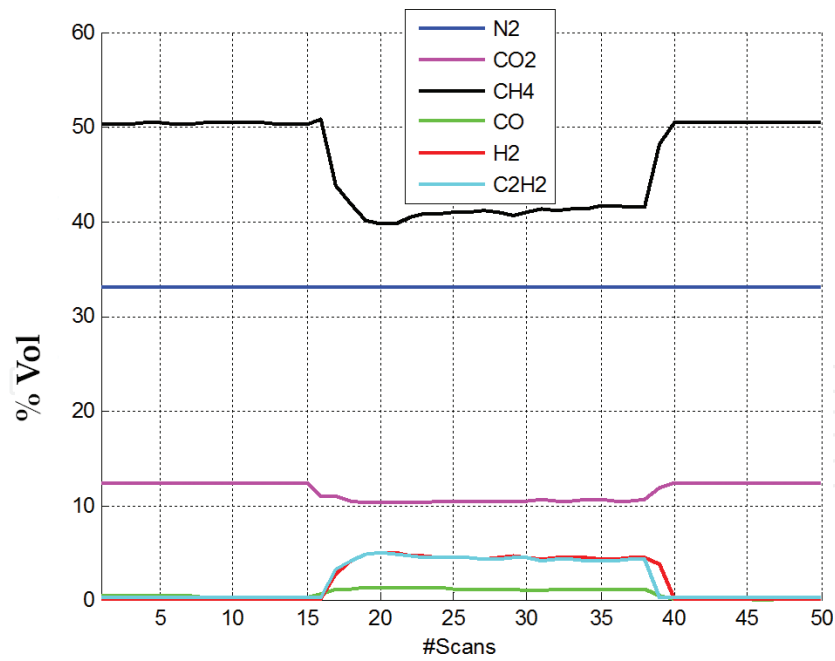


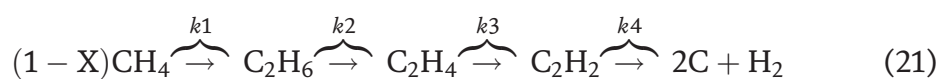
**Figure 8.**  
 Evolution concentration obtained by mass spectrometer.

Flow Rate LPM	Ein kJ	Conversion (%)		Yield/Selectivity (%)			SE (kJ/mol)	ECE (%)	Ref.
		CH <sub>4</sub>	CO <sub>2</sub>	H <sub>2</sub>	CO	C <sub>2</sub> H <sub>2</sub>			
2.52	72.57	90.20	77.11	17.27/ 19.20	60.25/ 75.72	19.13/ 21.32	1386	19.49	(a) This work
12	65.89	34.13	31.34	5.98/ 17.55	2.25/ 7.75	22.58/ 68.78	380.23	21.87	(b) This work
10	39.60	40.35	34.99	6.38/ 15.95	7.75/ 32.12	68.78/ 48.57	287.42	26.31	(c) This work
1.5	(270 W)	45	33	.../60	.../90	-/40	~600	~28	[31]
73.3	(18 kW)	78.71	64.80	.../82.85	.../96.8	///	///	57.22	[32]
4	(1.05 kW)	62.2	61.5	.../81.2	.../79.9	///	537	74.63	[33]
7.2	(400 W)	58.3	35.2	.../88.1	.../96.0	///	174	90.2	[34]

**Table 4.**  
 Operational conditions and numerical results in GEI treatment.

that is, 65.89 kJ. The result of the evolution of the concentration of the input and output species is shown in **Figure 8** with the corresponding numerical values expressed in **Table 4**, by using Eqs. (10)–(20). Real-time GHG study was carried out before and after the biogas by mass spectrometry by using a Cirrus 320 mass spectrometer.

A worth sub-product obtained is acetylene gas C<sub>2</sub>H<sub>2</sub>, normally obtained during methane pyrolysis at a temperature around 2150 K; thermodynamically this molecule is unstable relative to most other hydrocarbons at lower temperatures, but above 1500 K acetylene is more stable than other hydrocarbons, the reason why it is very used in high-quality welding applications. The most probable reforming path reaction for acetylene is described by the next reaction (21):





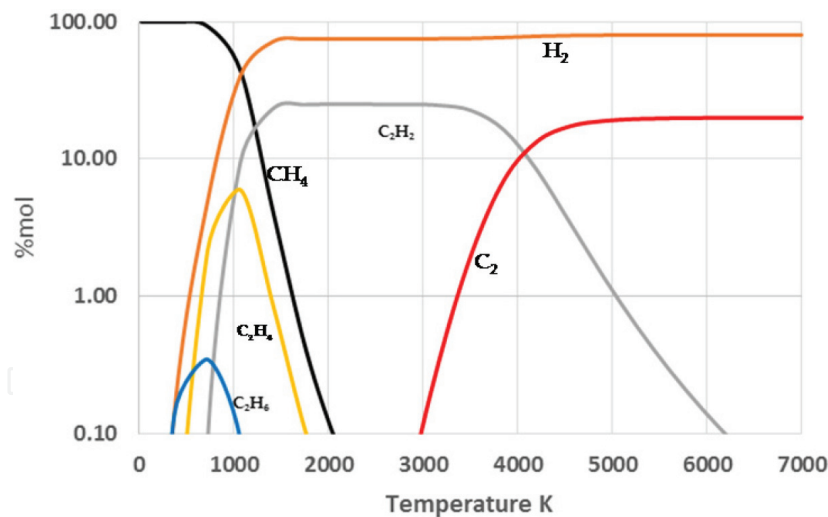
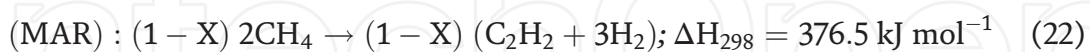


**Figure 9.**  
Yield of acetylene in methane plasma reforming.

being  $(1-X) \text{CH}_4$  the unconverted methane during GEI plasma reforming in (9). At high temperature, ethane ( $\text{C}_2\text{H}_6$ ) and ethylene ( $\text{C}_2\text{H}_4$ ) are very short-lived, being  $k_1$ ,  $k_2$ , and  $k_3$  rates constant with reaction times smaller than  $10^{-4}$  s [25, 26]; normally  $k_4$  is a rate constant with longer reaction time leading to  $\text{C}_2$  and  $\text{H}_2$  formation. Methane dissociation starts in warmer plasma zone, and the C–H bond breaks with simultaneous formation of  $\text{H}_3$ ,  $\text{CH}_2$ ,  $\text{CH}$ ,  $\text{H}$ ,  $\text{C}_2$ , and  $\text{C}$ ; the recombination of these radicals leads to the formation of acetylene through reactions (18) and (19).

**Figure 9** shows reaction (21) and its evolution concentration against temperature. The concentration level (% mol) is exposed in logarithmic scale to appreciate the ethane and ethylene concentration evolution which are much lower than that of acetylene, this previous being stable and remaining at a constant concentration up to 3500 K; beyond this temperature, acetylene is decayed into  $\text{H}_2$  and  $\text{C}_2$ . In warm plasma discharge, this average temperature is rarely attained, so the final by-products obtained are  $\text{H}_2$ ,  $\text{C}_2\text{H}_2$ , and  $\text{CO}$ .

The plasma dry reforming (DR) is not only described by Eq. (9); a complementary reaction succeeds and corresponds to a reaction occurring during  $\text{CO}_2 + \text{CH}_4$  reforming for methane that has not yet been converted into syngas. In this way, methane to acetylene reforming (MAR) in Eq. (22) can be established:



## 5. Conclusions

The aim of this work was focused in the GHG dissociation effectiveness by using a simple design of a warm plasma reactor applied for  $\text{CH}_4 + \text{CO}_2$  reforming obtaining competitive results, because dry reforming process efficiency possess very low SE and a relatively high ECE.

The warm plasma reactor has a compact size, faster response and reaction times, and cheaper than conventional gasification process because it requires no external ignition and neither cooling mechanism. Working at atmospheric pressure eliminates the operational and maintenance costs of vacuum equipment.

Concerning discharge stability and its frequency effect, a simple model based in an integro-differential equation in which the gas properties are all highly nonlinear function of temperature and pressure and its solution was resolved on the basis of simplifying assumptions.

Besides the syngas ( $\text{CO} + \text{H}_2$ ) a substantial formation of acetylene ( $\text{C}_2\text{H}_2$ ) is also obtained; therefore by-products with high energetic value are obtained.

The principal drawbacks were overcome using a special HF converter to get stable discharge and V-I linear behavior.

The plasma systems here proposed can be justified since it converts  $\text{CO}_2$  into harmless gases instead of storing  $\text{CO}_2$  in geological locations; it also has good energy conversions, with good treatment capacity and without generation of unwanted species. If the dissociation products can be used to produce a usable final product, such as syngas or other fuel gas, the technology becomes economically appealing.

## Acknowledgements


The authors would like to thank F. Ramos, M. Duran, M. Hidalgo, A. Romero, and J. Vences for their technical support. This work was supported under the grant 234737 from CONACYT.

## Author details

Joel O. Pacheco-Sotelo, Ricardo Valdivia-Barrientos\* and  
Marquidia Pacheco-Pacheco  
National Institute of Nuclear Research, Ocoyoacac, Mexico

\*Address all correspondence to: [ricardo.valdivia@inin.gob.mx](mailto:ricardo.valdivia@inin.gob.mx)

## IntechOpen

© 2019 The Author(s). Licensee IntechOpen. This chapter is distributed under the terms of the Creative Commons Attribution License (<http://creativecommons.org/licenses/by/3.0/>), which permits unrestricted use, distribution, and reproduction in any medium, provided the original work is properly cited. 

## References

- [1] Jiang Z, Xiao T, Kuznetsov VL, Edwards PP. Turning carbon dioxide into fuel Phil. Philosophical Transactions of the Royal Society A. 2010;**368**:3343-3364. Downloaded from <http://rsta.royalsocietypublishing.org/> [April 7, 2016]
- [2] Kolasinski WK. Frontiers of surface science. Current Opinion in Solid State & Materials Science. 2006;**10**:129-1312. DOI: 10.1016/j.cossms.2007.04.002
- [3] Bose BK. Global warming; energy, environmental pollution, and the impact of power electronics. IEEE Industrial Electronics Magazine. 2010;**4**:6-17. DOI: 10.1109/MIE.2010.935860
- [4] Greenhouse Gas Emissions and Atmospheric Concentrations have Increased over the Past 150 Year. [https://www.eia.gov/energyexplained/index.php?page=environment\\_how\\_ghg\\_affect\\_climate](https://www.eia.gov/energyexplained/index.php?page=environment_how_ghg_affect_climate)
- [5] Swingedouw D, Mignot J, Guilyardi É, Nguyen S, Ormières L. Tentative reconstruction of the 1998–2012 hiatus in global temperature warming using the IPSL–CM5A–LR climate model. Comptes Rendus Geoscience. 2017;**349**: 369-379
- [6] Emission Rates and Concentration of Greenhouse Gases, Chapter 11, The National Academies of Sciences Engineering medicine (NAP) <https://www.nap.edu/read/1605/chapter/15>. 1992: pp. 91-99
- [7] Schloegl F. The solar refinery. In: Schlögl R, editor. Chemical Energy Storage. de Gruyter. 2013
- [8] Elshout PMF, van Zelm R, Balkovic J, Obersteiner M, Schmid E, Skalsky R, van der Velde M, Huijbregts MAJ. Greenhouse-Gas Payback Times for Crop-Based Biofuels. Available from: [https://www.researchgate.net/publication/276459527\\_Greenhouse-gas\\_payback\\_times\\_for\\_crop-based\\_biofuels](https://www.researchgate.net/publication/276459527_Greenhouse-gas_payback_times_for_crop-based_biofuels)
- [9] Cárdenas Barrañón DC. Methanol and Hydrogen Production: Energy and Cost Analysis [Master thesis]. Luleå, Sweden: Department of Applied Physics, Mechanical and Material Engineering, Luleå University of Technology; 2006. ISSN: 1653-0187
- [10] Gallagher MJ, Geiger R, Polevich A, Rabinovich A, Gutsol A, Fridman A. On-board plasma-assisted conversion of heavy hydrocarbons into synthesis gas. Fuel. 2010;**89**:1187-1192
- [11] Schloegl F. The solar refinery, in: Chemical Energy Storage, Robert Schloegl Editor. de Gruyter; 2013. [http://www.chemistry-software.com/v9\\_SIM-PROCESS%20SIMULATION.html](http://www.chemistry-software.com/v9_SIM-PROCESS%20SIMULATION.html)
- [12] Aubreton J, Elchinger M-F, Hacalaand A, Michon U. Transport coefficients of typical biomass equimolar CO–H<sub>2</sub> plasma. Journal of Physics D: Applied Physics. 2009;**42**: 095206
- [13] Heijkers S et al. CO<sub>2</sub> conversion in a microwave plasma reactor in the presence of N<sub>2</sub>: Elucidating the role of vibrational levels. The Journal of Physical Chemistry. 2015;**119**(23): 12815-12828
- [14] Berthelot A, Bogaerts A. Modeling of CO<sub>2</sub> splitting in a microwave plasma: How to improve the conversion and energy efficiency. The Journal of Physical Chemistry. 2017;**121**(15): 8236-8251
- [15] Long H, Shang S, Tao X, Yin Y, Dai X. CO<sub>2</sub> reforming of CH<sub>4</sub> by combination of cold plasma jet and Ni/Al<sub>2</sub>O<sub>3</sub> catalyst. International Journal of Hydrogen Energy. 2008;**33**(3):5510-5515

- [16] Frances L. The study of CO<sub>2</sub> conversion in a microwave plasma/catalyst system [PhD dissertation]. Ann Arbor, MI, USA: Department of Aerospace Engineering, University of Michigan; 2012
- [17] Fabela JLT et al. Electrical model for HPS discharge based on the energy-balance equation. *IEEE Transactions on Plasma Science*. 2007;**35**(3):637-643
- [18] Waymouth JF. *Electric Discharge Lamps*. Cambridge, MA, USA: MIT Press; 1971
- [19] Boulos MI, Fauchais P, Pfender E. *Thermal Plasmas Fundamentals and Applications*. Vol. 1. New York, NY, USA: Plenum Press; 1974
- [20] de Groot J, van Vliet J. *The High Pressure Sodium Lamp*. Deventer, The Netherlands: Macmillan Education; 1986. pp. 98-127
- [21] Chamam A. *Etude de Decharges Haute Pression et Mercure Halogenure Alimentees par des Courants Rectangulaires et Pulses* [PhD dissertation]. Toulouse, France: University Paul Sabatier Toulouse; 2005
- [22] Dakin JT, Rautenberg TH Jr. Frequency dependence of the pulsed high pressure sodium arc spectrum. *Journal of Applied Physics*. 1984;**56**(1):118-124
- [23] Tao X, Bai M, Li X, Long H, Shang S, Yin Y, et al. CH<sub>4</sub>-CO<sub>2</sub> reforming by plasma-challenges and opportunities. *Progress in Energy and Combustion Science*. 2011;**37**(2):113-124
- [24] Tamosiunas A, Valatkevicius P, Valincius V, Grigaitiene V. Production of synthesis gas from propane using thermal water vapor plasma. *International Journal of Hydrogen Energy*. 2014;**39**:2078-2086
- [25] Holman A, Rokstad O, Solbakken A. High-temperature pyrolysis of hydrocarbons. 1. Methane to acetylene. *Industrial and Engineering Chemistry Process Design and Development*. 1976;**15**(3):439-444
- [26] Liu C, Mallinson R, Lobban L. Non-oxidative methane conversion to acetylene over zeolite in a low temperature plasma. *Journal of Catalysis*. 1998;**179**:326-333
- [27] Huang J, Zou J, Winston WS. CO<sub>2</sub> selective membranes for hydrogen fuel processing, Chapter 9. In: Liu K, Song C, Subramani V, editors. *Hydrogen and Syngas Production and Purification Technologies*. Hoboken, New Jersey: John Wiley & Sons, Inc.; 2010
- [28] Albo J, Alvarez-Guerra M, Castaño P, Irabien A. Towards the electrochemical conversion of carbon dioxide into methanol. *Green Chemistry*. 2015;**17**(4):2305-2324
- [29] Pacheco J et al. Greenhouse gas treatment and H<sub>2</sub> production, by warm plasma reforming. *International Journal of Hydrogen Energy*. 2015;**40**(48):17165-17171. DOI: 10.1016/j.ijhydene.2015.08.062
- [30] Ravasio S, Cavallotti C. Analysis of reactivity and energy efficiency of methane conversion through non thermal plasmas. *Chemical Engineering Science*. 2012;**84**:580-590
- [31] Indarto A, Choi JW, Lee H, Song HK. Effect of additive gases on methane conversion using gliding arc discharge. *Energy*. 2006;**31**(14):2986-2995
- [32] Tao X, Bai M, Wu Q, Huang Z, Yin Y, Dai X. CO<sub>2</sub> reforming of CH<sub>4</sub> by binode thermal plasma. *International Journal of Hydrogen Energy*. 2009;**34**:9373-9378
- [33] Ni G, Lan Y, Cheng C, Meng Y, Wang X. Reforming of methane and carbon dioxide by DC water plasma at atmospheric pressure. *International*

Journal of Hydrogen Energy. 2011;**36**  
(20):12869-12876

[34] Lin Q, Ni G, Guo Q, Wu W, Li L,  
Zhao P, Xie H, Meng Y. Reforming of  
CH<sub>4</sub> and CO<sub>2</sub> by Combination of  
Alternating Current-Driven  
Nonthermal Arc Plasma and Catalyst.  
IEEE Transactions on Plasma Science.  
2007;**46**(7):2528-2535

IntechOpen

IntechOpen